Unsteady Supersonic Aerodynamic Theory by the Method of Potential Gradient

William P. Jones*
Texas A&M University, Texas

and

Kari Appa†
Bell Aerospace Textron, Buffalo, New York

A generalized solution of the hyperbolic wave equation has been derived by one of the authors. The method used has been further developed to relate the velocity components at a field point to the potential gradient distribution in the dependence domain. Singular integrals have been evaluated in closed form, whereas numerical integration methods are suggested for treating more complex but analytic functions. Idealization of the lifting surfaces by trapezoidal elements with two sides parallel to the streamlines is computationally efficient because line integrations along the other two sides need only be considered. Furthermore, all the integrands vanish on the Mach cone and the need for determining the hyperbolic curves of intersection of the cone with the lifting surface is avoided. Generalized aerodynamic coefficients for three AGARD planforms have been calculated and compared with the available results.

Nomenclature

k,k'	= reduced frequencies, $\omega\ell/U$, kM/β
$2\pi K$	= modified potential difference across the lifting surface
ℓ	= reference length
$\hat{\ell},\hat{m},\hat{n}$	= direction cosines of a normal
$\tilde{\ell}$	= local lift
m	= slope of a line
M	= Mach number
q	= $\frac{1}{2}\rho U^2$ dynamic pressure
Q_{IJ}	= generalized aerodynamic coefficients = $Q_{ij}/q\ell^3$
S	= surface of integration
r^2	= $(X_0-X)^2-(Z_0-Z)^2$
R^2	= hyperbolic radius squared = $r^2-(Y_0-Y)^2$
t	= dimensional time
T	= nondimensional time
U	= airstream velocity
u,v,w	= induced velocity components, also termed as backwash, sidewash, and normalwash components
W	= influence coefficient matrix relating normal velocity and velocity doublets [Eq. (41)].
x,y,z	= dimensional space coordinates
X,Y,Z	= nondimensional space coordinates
α	= constant of a line
β	= $\sqrt{M^2-1}$
η_D	= displacement normal to the lifting surface
η	= Y_0-Y
ξ	= X_0-X
ρ	= air density
ϕ	= velocity potential, a scalar quantity
Φ	= $\phi e^{ik'Mx}$ modified potential
ω	= circular frequency of harmonic motion, rps

Introduction

ACCURATE determination of unsteady aerodynamic forces is essential for precise evaluation of the aeroelastic stability characteristics of flight vehicles. In the subsonic case, the integral formulation is simple and computational methods have been well developed.[2] In the supersonic case, the problem is complicated by the fact that pressure discontinuities arise because of the conical flowfield emanating from geometric irregularities, such as cranked leading edges, wing tips, interfering/interacting surfaces, etc. A total solution for such problems by closed-form methods has not yet been found. Hence, superposition methods of finite-element type, using sources, velocity potential doublets, or pressure doublets as basic variables have received attention in the literature.

The source superposition method gives a very simple direct integral relationship between the potential and the downwash field (which is determined by the mode shapes) in the noninteracting case.[3] However, in the interacting case, the potential is first related to the source strength, and this is in turn related to the downwash distribution.[4] Thus, by this method, two sets of equations are required to solve the problem. In addition, integration over wake regions and nonunique "diaphragms" is necessary as a part of the solution.

In the velocity-potential method, there is a direct relationship between the downwash (the mode shapes) and the velocity potential.[1] Diaphragm regions are no longer necessary and the wake regions do not need detailed modeling since their behavior is determined by the trailing edge potentials of the wake-producing surface. The integral relations, which are more complicated than in the source superposition method, have been considerably simplified in the current work.

The pressure potential or kernel function method is a "direct" approach via a relation between downwash and pressures and aerodynamic coefficients.[5-8] This integral relation is, however, even more complicated than in the velocity-potential approach.

For arbitrary configurations, the numerical methods employed may broadly be classified as collocation and finite element methods. Collocation methods assume, *a priori*, certain mode shapes or series expansions of the unknown parameters such as pressure and doublet strengths. The coefficients of these series or modes are determined from a set of algebraic equations established by satisfying the integral relation only at an appropriate number of collocation points. The number of equations is comparatively few and an ef-

Received May 17, 1976; revision received Oct. 13, 1976.

Index categories: Supersonic and Hypersonic Flow; Aeroelasticity and Hydroelasticity.

*Emeritus Professor, Dept. of Aerospace Engineering. Fellow AIAA.

†Chief, Dynamic Analysis. Member AIAA.

ficient computation generally results for simple configurations.[9] In a recent paper, Cunningham[10] uses the three-dimensional kernel function with a judicious selection of pressure functions for interacting surface configurations.

However, the application of pressure-collocation methods to handle general configurations is complicated by the difficulty of choosing pressure modes for complex multidimensional configurations such as wing-body combinations.

In finite element methods, the integration over the dependence domain is replaced by a sum of integrations over a number of simple elemental domains (finite elements). Over each area element, the unknown parameter is expressed as a sum of simple functions. A number of finite element shapes have been used, such as squares, Mach or characteristic boxes, and triangular or quadrilateral elements. Numerical approaches differ also in the choice of functional variation within each element and in the integration methods over the element.[11-20]

In Mach or characteristic box schemes, planform edges have usually been approximated by jagged representations that result in erratic behavior of the pressure over the whole surface. More recent versions of Mach box programs are described in Refs. 11 and 12.

Stark[13] used elementary characteristic boxes in developing a digital computer program in which special consideration was given to the handling of subsonic singular leading edges. These modifications, however, detract very significantly from the basic simplicity of the Mach or charactertistic box approach, the computational price paid for additional accuracy being large.

A triangular representation of the dependence domain using a linear distribution of sources was developed in Refs. 14 and 15. This method offers acceptable accuracies with far fewer elements than other methods.

Allen and Sadler[17] using characteristic elements, developed a doublet superposition method based on Jones' integrated potential formulation for planar configurations. They expressed the kernel (sine and cosine) functions as parabolic interpolation functions within each element. Woodcock and York[18] extended this approach to interacting wing and wing-body configurations.

The integrated potential approach was further developed in Ref. 23, using linearly varying potential doublets within triangular elements. Closed-form integrals were employed to evaluate the singular functions, whereas numerical integration methods were adopted for more complex but analytic functions.

Although good results were obtained with fewer elements, an arbitrary wing with a control surface could not satisfactorily be idealized. This disadvantage of the velocity-potential method led to the development of the potential-gradient method, which is described in this paper. In this scheme, the potential gradient in the stream direction is considered as an independent variable and is assumed to be constant over an element. This results in fewer integrals than in the velocity-potential method discussed in Ref. 23. Once again closed-form integrals have been obtained for singular functions and recurrence formulae derived for nonsingular terms. Since two sides of a typical quadrilateral element are parallel to the stream, the computational efficiency is further increased as the integrals along these two lines and along the boundary of the area of the wing cut by the Mach cone vanish. Velocity-potential distributions and generalized aerodynamic coefficients have been obtained by the use of the potential-gradient method and compared with available results derived by other methods.

General Analysis

In the present analysis, the coordinates $x, y,$ and z and time t are replaced in nondimensional form by $X, Y, Z,$ and T, respectively, where

$$X = x/\ell\beta \quad Y = y/\ell \quad Z = z/\ell \quad T = Ut/\ell \tag{1}$$

ℓ being the standard length, U the airspeed, and $\beta = [M^2 - 1]^{1/2}$, where M is the Mach number. The effect of the above transformation is to change the planform of the wing in such a way that its chord is lengthened while its lateral dimensions remain the same. At the same time the Mach lines in the X, Y, Z coordinate system are inclined at $\pm 45°$ to the X axis as indicated in Fig. 1.

Next, let us suppose that a delta wing with subsonic leading edges is oscillating in the airstream with frequency ω rps. Then if ϕ, the velocity potential of the disturbed flow, is replaced by a nondimensional modified potential Φ such that

$$\Phi = (\phi/U\ell)\, e^{ikM^2X/\beta} \tag{2}$$

it can be proved that

$$\frac{\delta^2\Phi}{\delta X^2} - \frac{\delta^2\Phi}{\delta Y^2} - \frac{\delta^2\Phi}{\delta Z^2} + k'^2\Phi = 0 \tag{3}$$

where $k' = kM/\beta$ and $k = \omega\ell/U$. Furthermore, it is shown in Ref. 1 that the solution of Eq. (3) may be derived using the integral relation

$$\Phi(X_0, Y_0, Z_0) = -\frac{\delta}{\delta Z_0}\int\int K(X,Y)\,\frac{\cos k'R}{R}\,\mathrm{d}X\mathrm{d}Y \tag{4}$$

where the integral is taken over the part of the wing cut off by the Mach cone with vertex at X_0, Y_0, Z_0. The symbol $K \equiv (\Phi_a - \Phi_b)/2\pi$ denotes the difference between the modified velocity potential above and below the wing and

$$R = [(X_0 - X)^2 - (Y_0 - Y)^2 - (Z_0 - Z)^2]^{1/2} \tag{5}$$

The surface of the Mach cone with vertex at X_0, Y_0, Z_0 is defined by $R = 0$ and the mean position of the wing is assumed to be in the plane $Z = 0$.

In general, the modes of motion of the wing are assumed to be known. The displacement normal to the wing's surface is usually denoted by $\eta_D\,[\equiv \ell\bar{\eta}\exp(ikT)]$, where $\bar{\eta}$ is a function of x and y. The condition for tangential flow over the wing may then be expressed as

$$\frac{\mathrm{d}\bar{\eta}_D}{\mathrm{d}t} = \frac{\delta\phi}{\delta n}$$

or

$$\frac{\mathrm{d}\bar{\eta}}{\mathrm{d}T} = \left[\frac{\hat{\ell}}{\beta}\frac{\delta}{\delta X_0} + \hat{m}\frac{\delta}{\delta Y_0} + \hat{n}\frac{\delta}{\delta Z_0}\right](\Phi e^{-ik'MX}) \tag{6}$$

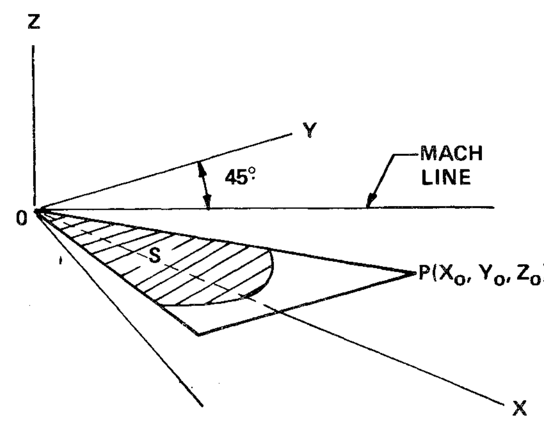

Fig. 1 Domain of influence in supersonic flow.

where

$$\mathrm{d}\bar{\eta}/\mathrm{d}T = ik\bar{\eta} + (1/\beta)(\delta\bar{\eta}/\delta X)$$

and $\delta\phi/\delta n$ is the velocity normal to the surface induced by the doublet distribution over the wing and the wake. The factor $\exp(ikT)$ has been omitted in Eq. (6) and throughout the analysis.

When the wing lies approximately in the plane $z=0$ and the displacement η_D is small, the above relation simplifies. In terms of the modified potential Φ and the nondimensional coordinates defined by Eq. (1), the boundary condition to be satisfied at a typical point X_0, Y_0, Z_0 is then obtained by differentiating Eq. (4). For the case considered, Eq. (6) is replaced by

$$\frac{\delta\Phi}{\delta Z_0} = \left[ik\bar{\eta} + \frac{1}{\beta}\frac{\delta\bar{\eta}}{\delta X_0}\right] e^{ik'MX_0} \tag{7a}$$

$$= -\frac{\delta^2}{\delta Z_0{}^2}\int\int K(X,Y)\frac{\cos k'R}{R}\,\mathrm{d}X\mathrm{d}Y \tag{7b}$$

When the appropriate K distribution that satisfies the above equation has been determined, the values of $\delta\Phi/\delta X_0$ and $\delta\Phi/\delta Y_0$ can be deduced from Eq. (4) by differentiation. The actual velocity components $\delta\phi/\delta X_0$, $\delta\phi/\delta Y_0$ may then be derived by differentiating Eq. (2).

The Modified Upwash

To determine the modified velocity components, it is convenient to express $\cos k'R$ in series form so that

$$\frac{\cos k'R}{R} = \sum_{n=0}^{N} C_{2n} R^{2n-1} \tag{8}$$

where

$$C_{2n} = (-1)^n k'^{2n}/2n! \tag{9}$$

The modified upwash W is then given by

$$W = \frac{\delta\Phi}{\delta Z_0} = \sum C_{2n} W_{2n} \tag{10}$$

where

$$W_{2n} = -\frac{\delta^2}{\delta Z_0{}^2}\int\int K(x,Y) R^{2n-1}\mathrm{d}X\mathrm{d}Y \tag{11}$$

and $n=0,1,2,$ etc. When $n=0$ and $Z=0$,

$$W_0 = -\frac{\delta^2}{\delta Z_0{}^2}\int\int \frac{K}{R}\mathrm{d}\xi\mathrm{d}\eta \tag{12}$$

where $\xi = X_0 - X$ and $\eta = Y_0 - Y$. By integrating by parts, it may be deduced that

$$W_0 = \frac{\delta^2}{\delta Z_0{}^2}\int\int_S \frac{\delta K}{\delta\xi} L\mathrm{d}\xi\mathrm{d}\eta \tag{13}$$

where

$$L = \frac{1}{2}\log_e\left(\frac{\xi+R}{\xi-R}\right) \tag{14}$$

Let us next assume that the area of integration S is divided into a number of small quadrilateral elements E with chordwise sides parallel to the ξ or X axis. It is further supposed that $\delta K/\delta\xi\,(=-\delta K/\delta X)$ is constant over each element. Then, since $L=0$ over the part of the boundary of S on the surface of the cone $R=0$, it can be deduced that W_0 is given approximately by

$$W_0 = \sum_E \frac{\delta K}{\delta X}\frac{\delta}{\delta Z_0}\int\int_S \frac{Z_0}{\eta^2+Z_0{}^2}\left(\frac{\xi}{R}\right)\mathrm{d}\xi\mathrm{d}\eta \tag{15}$$

the sum of the contributions from all the E elements. The above equation, after integration with respect to ξ, then yields

$$W_0 = \sum \frac{\delta K}{\delta X}\oint \frac{\delta}{\delta Z_0}\left(\frac{Z_0 R}{\eta^2+Z_0{}^2}\right)\mathrm{d}\eta \tag{16}$$

where $\oint$ denotes the contour integral around a quadrilateral element in the anticlockwise direction as indicated in Fig. 2. In Eq. (16), ξ is replaced by $m\eta+\alpha$ where m and α have the values corresponding to the particular side of the quadrilateral over which the integration is being performed and

$$R = [(m^2-1)\eta^2 + 2m\alpha\eta + \alpha^2 - Z_0{}^2]^{1/2} \tag{17}$$

It should be noted that m^2-1 can be negative and that $\alpha^2 \geq Z_0{}^2$. When the above expression for R is substituted into Eq. (16), it can be shown that

$$W_0 = -\sum_E \frac{\delta K}{\delta X} I_0 \tag{18}$$

The integral I_0 is then given by

$$I_0 = [(R\eta/(\eta^2+Z_0{}^2)) - (m^2-1)F_0 + m^2 Z_0^2 F_1 - m\alpha F_2]_C \tag{19}$$

where

$$F_0 = \oint \mathrm{d}\eta/R \tag{20a}$$

$$F_1 = \oint \mathrm{d}\eta/(\eta^2+Z_0{}^2)R \tag{20b}$$

$$F_2 = \oint \eta\mathrm{d}\eta/(\eta^2+Z_0{}^2)R \tag{20c}$$

Since

$$\frac{\mathrm{d}L}{\mathrm{d}\eta} = \frac{mZ_0{}^2 - \eta\alpha}{(\eta^2+Z_0{}^2)R} \tag{21}$$

it follows that the value of F_2 could be derived from the relation

$$\alpha F_2 = mZ_0{}^2 F_1 - L \tag{22}$$

Hence, only F_0 and F_1 need be evaluated. It can readily be deduced that

$$F_0 = \frac{1}{(m^2-1)^{1/2}}\log_e\frac{(m^2-1)^{1/2}R + (m^2-1)\eta + m\alpha}{m^2-1}, \quad m>1 \tag{23a}$$

$$F_0 = \frac{1}{(1-m^2)^{1/2}}\sin^{-1}\frac{(1-m^2)\eta - m\alpha}{[\alpha^2 - Z_0{}^2(1-m^2)]^{1/2}}, \quad m<1 \tag{23b}$$

$$F_0 = \frac{R}{\alpha} \qquad m=1 \tag{23c}$$

The integral F_1 can be also be derived by substituting $\eta = Z_0 \tan(\theta+\gamma)$ in the integrand and putting $\tan\gamma = mZ_0/\alpha$. After some reduction, the required formula can be shown to be

$$F_1 = \frac{1}{Z_0(\alpha^2 + m^2 Z_0{}^2)} \left[\alpha \sin^{-1} \frac{\eta\alpha - mZ_0{}^2}{\{(\eta^2+Z_0{}^2)[\alpha^2+Z_0^2(m^2-1)]\}^{1/2}} + \frac{mZ_0}{2}\log_e \frac{(\xi+R)}{(\xi-R)}\right]_{\eta_1}^{\eta_2} \tag{24}$$

where the integral is taken along the line $\xi = m\eta + \alpha$ from η_1 to η_2. It should be noted that the values of m and α are different for the lower side of the quadrilateral element.

When the values of all the F integrals over the upper and lower sides of each element have been determined, the total integral I_0 for any element can be evaluated. From Eq. (18) the upwash due to all the elements may then be obtained by summation.

Similarly, it can be deduced that

$$W_2 = \frac{\delta}{\delta Z}\int\int \frac{KZ_0 \mathrm{d}\xi}{R}\mathrm{d}\eta \tag{25a}$$

$$W_2 = \sum \frac{\delta K}{\delta X}\oint\left(\xi L - R - \frac{Z_0{}^2 R}{\eta^2+Z_0{}^2}\right)\mathrm{d}\eta \tag{25b}$$

$$W_2 = \sum_E \frac{\delta K}{\delta X} I_2(\eta) \tag{25c}$$

where

$$I_2(\eta) = \left[\frac{\eta L(m\eta+2\alpha)}{2} - \frac{R\eta}{2} + \frac{F_0}{2}[\alpha^2 - 3(m^2-1)Z_0^2] + \frac{Z_0^2 F_1}{2}(3mZ_0^2 - 4\alpha^2) - \frac{7m\alpha Z_0^2 F_2}{2}\right]_C \tag{26}$$

is taken around the contour C of each element of area (Fig. 2). The corresponding formula for W_{2n} term, for $n \geq 2$ is given by

$$W_{2n} = (2n-1)\sum \frac{\delta K}{\delta X} I_{2n} \tag{27}$$

where

$$I_{2n} = \oint (H_{2n-2} - (2n-3)Z_0{}^2 H_{2n-4})\mathrm{d}\eta \tag{28}$$

in which

$$H_{2n} = \frac{R^{2n+1}}{2n(2n+1)} - \frac{(2n-1)}{2n}(\eta^2+Z_0{}^2)H_{2n-2} \tag{29}$$

with

$$H_0 = \xi L - R \tag{30}$$

and

$$H_2 = (R^3/6) - (\eta^2 + Z_0{}^2)H_0/2 \tag{31}$$

The integrand in I_{2n} is analytic throughout the dependence domain and closed-form integration is possible. However, it is more economical to evaluate the integral numerically, say by the method of Gaussian quadrature. It is clear from the expressions for H_{2n} that the integrals I_{2n} vanish on the Mach boundary. This eliminates the need for the determination of the intersection of the dependent domain by the Mach hyperbola.

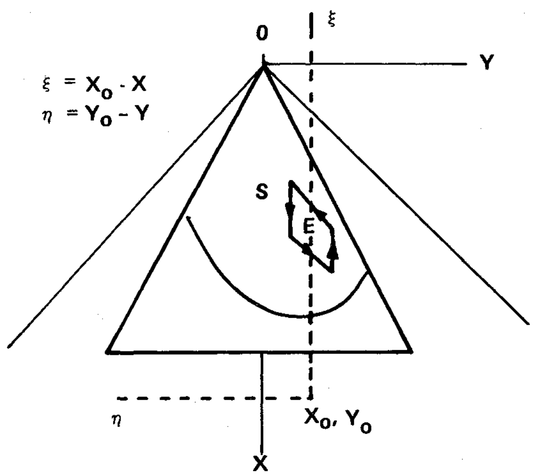

Fig. 2 Contour integration along discrete elements.

Modified Backwash and Sidewash Components

The corresponding velocity components U_{2n}, V_{2n} along the $0X$ and $0Y$ axis, respectively, may also be deduced.

It can readily be proved that

$$\frac{\delta\Phi_0}{\delta X_0} = U_0 = Z_0 \sum \frac{\delta K}{\delta X}(mF_2 + \alpha F_1) \tag{32}$$

$$\frac{\delta\Phi_2}{\delta X_0} = U_2 = Z_0 \sum \frac{\delta K}{\delta X}(\eta L - mZ_0^2 F_2 - \alpha Z_0^2 F_1 + \alpha F_0) \tag{33}$$

and

$$\frac{\delta\Phi_{2n}}{\delta X_0} = U_{2n} = (2n-1)Z_0 \sum \frac{\delta K}{\delta X}\oint P_{2n-2}\mathrm{d}\eta \quad n \geq 2 \tag{34}$$

where P_{2n} is defined by

$$P_{2n} = \int R^{2n-1}\mathrm{d}\eta = [\xi R^{2n-1} - (2n-1)(\eta^2+Z_0^2)P_{2n-2}]/2n \tag{35}$$

with

$$P_0 = L \tag{36}$$

and

$$P_2 = [\xi R - (\eta^2 + Z_0^2)L]/2 \tag{37}$$

Similarly, the sidewash components are given by

$$\frac{\delta\Phi_0}{\delta Y_0} = V_0 = +Z_0 \sum \frac{\delta K}{\delta X}\left(\frac{R}{\eta^2+Z_0{}^2}\right) \tag{38}$$

$$\frac{\delta\Phi_2}{\delta Y_0} = V_2 = +Z_0 \sum \frac{\delta K}{\delta X}[(m\eta+\alpha)L - R] \tag{39}$$

and

$$\frac{\delta\Phi_{2n}}{\delta Y_0} = V_{2n} = +(2n-1)Z_0 \sum \frac{\delta K}{\delta X} H_{2n-2}, \quad n \geq 2 \tag{40}$$

Finally the modified normal distribution using Eq. (6) may be expressed in matrix form

$$\frac{\mathrm{d}\bar{\eta}}{\mathrm{d}T_0} e^{ik'MX_0} = \left[W\right]\left\{\frac{\delta K}{\delta X}\right\} \tag{41}$$

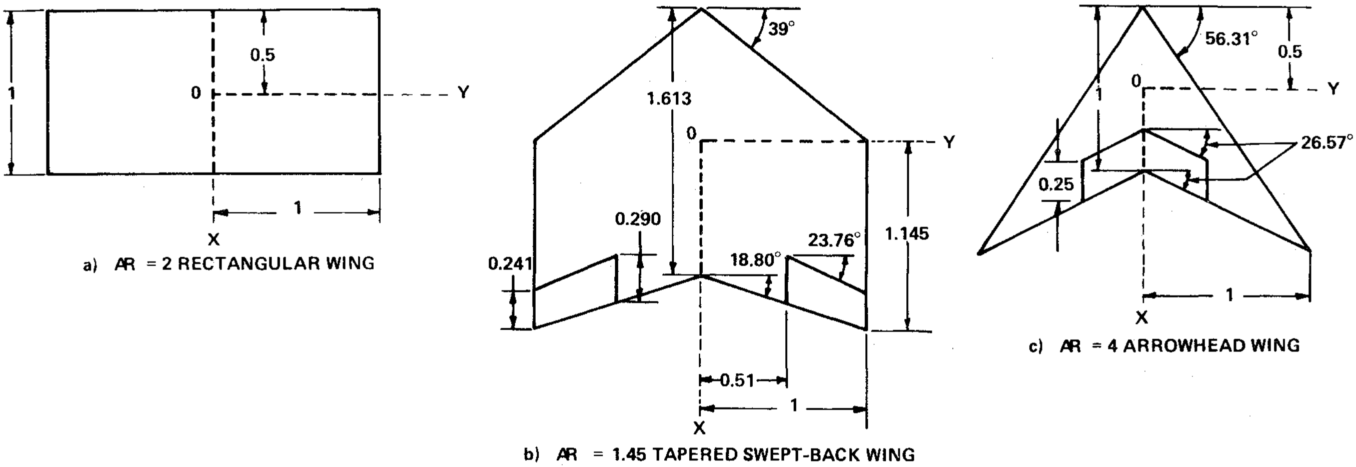

Fig. 3 AGARD planforms.

Calculation of the Generalized Forces

Since $d\bar{\eta}/dT_0$ is known over the wing, the solution of Eq. (41) is given simply by

$$\left\{\frac{\delta K}{\delta X}\right\}=\left[W\right]^{-1}\frac{d\bar{\eta}}{dT_0} \qquad (42)$$

The column on the left gives the gradients of K in the stream direction at various points over the wing. It should also be remembered that $K=0$ along its leading edges.

The lift on an element $dxdy$ of the wing's surface is denoted by $\ell(x,y)\exp(ikT)$ and hence

$$\ell(x,y)\,dxdy=\ell^2\beta\tilde{\ell}(X,Y)\,dXdY \qquad (43)$$

where the lift distribution

$$\tilde{\ell}(X,Y)=2\pi\frac{\rho U^2}{\beta}\left[\frac{\delta K}{\delta X}-\frac{ikK}{\beta}\right]e^{-ik'MX} \qquad (44)$$

By the principle of virtual work, the generalized aerodynamic influence coefficient (AIC) can be written as

$$Q_{ij}=4\pi q\ell^3\tilde{Q}_{ij} \qquad (45)$$

where $\tilde{Q}_{ij}$ is the nondimensional form of the coefficients defined by

$$\tilde{Q}_{ij}=\sum_E\bar{\eta}_i\left(\frac{\delta K_j}{\delta X}-i\frac{k}{\beta}K_j\right)A_je^{-ik'MXj} \qquad (46)$$

In the previous equation, A_j is the area of a quadrilateral element of the wing and the contributions from all such elements of both sides of the wing are summed. The required values of K_j are readily derived by integration once the distribution of $\delta K_j/\delta X$ over the wing has been found

Wake Field

In the wake, since it can sustain no lift,

$$(\delta K/\delta X)-i(k/\beta)K=0$$

Table 1 AGARD rect. wing (planform Fig. 3a) modes $Z_1=1.0$ $Z_2=x\text{-}C/2$ $AR=2.0$

Mach No.	Methods (Matrix or Sp/Ch Pts.)[a]	Qij	k=0 Re(Q)	k=0 Im(Q)	k=0.3 Re(Q)	k=0.3 Im(Q(	k=0.6 Re(Q)	k=0.6 Im(Q)
	δφ/δx(49)				0.215	1.070	0.472	1.715
	M9(34/26)[b]	1,1			0.205	1.060	0.749	1.820
	M19(22/17)[c]				0.189	1.009	0.348	1.639
	δφ/δx		3.978		3.567	−0.593	2.938	−0.556
	M9	1,2	3.951		3.531	−0.545	3.058	−0.946
1.2	M19		3.750		3.370	−0.500	2.840	−0.294
	δφ/δx				−0.001	−0.132	−0.096	−0.300
	M9	2,1			−0.005	−0.141	−0.026	−0.310
	M19				−0.005	−0.131	−0.107	−0.285
	δφ/δx		−0.370		−0.419	0.157	−0.403	0.440
	M9	2,2	−0.398		−0.446	−0.177	−0.427	0.350
	M19		−0.368		−0.411	−0.165	−0.380	0.450
	δφ/δx(99)				0.008	1.128	0.158	2.065
	M9(34/54)[b]				0.034	1.144	0.146	2.083
	M19(14/22)[c]	1,1			0.019	1.088	0.124	1.997
	δφ/δx		3.880		3.955	0.255	3.781	−0.035
	M9	1,2	3.787		4.0	0.088	3.806	0.004
1.05	M19		3.542		3.80	0.134	3.648	0.036
	δφ/δx				−0.200	−0.193	−0.3419	−0.200
	M9	2,1			−0.185	−0.204	−0.333	−0.251
	M19				−0.174	−0.197	−0.320	−0.244
	δφ/δx		−1.339		−0.544	0.837	−0.1616	0.797
	M9	2,2	−1.363		−0.590	0.790	−0.250	0.825
	M19		−1.293		−0.571	0.749	−0.247	0.790

[a]Spanwise and chordwise grid points. [b]As reported in Ref. 21 using the method of Ref. 22. [c]As reported in Ref. 21 using the method of Ref. 13.

Table 2 AGARD swept wing (planform Fig. 3b) modes $Z_1 = 1.0$ $Z_2 = x\text{-}CR/2$ $AR = 1.45$

Mach No.	Methods (Matrix or *Sp/Ch* Pts)[a]	*Qij*	$k=0$ *Re(Q)*	$k=0$ *Im(Q)*	$k=0.5$ *Re(Q)*	$k=0.5$ *Im(Q)*
	$\delta\phi/\delta x$(49)				0.0343	2.0558
	M9(34/51)[b]	1,1			0.0110	1.740
	M19(20/30)[c]				−0.0228	1.675
	$\delta\phi/\delta x$		4.181		4.4195	0.5875
	M9	1,2	4.140		3.811	0.8380
1.2	M19		3.930		3.671	0.8660
	$\delta\phi/\delta x$				−0.2485	0.1070
	M9	2,1			−0.2780	0.0205
	M19				−0.283	0.0040
	$\delta\phi/\delta x$		+0.0430		0.4342	1.122
	M9	2,2	0.0590		0.287	1.245
	M19		−0.0120		0.244	1.229
	$\delta\phi/\delta x$				0.0775	1.278
	M9				0.0720	1.305
	M19	1,1			0.0599	1.263
	$\delta\phi/\delta x$		2.732		2.557	0.1843
	M9	1,2	2.716		2.617	0.2490
M = 2.0	M19		2.624		2.533	0.2566
	$\delta\phi/\delta x$				0.0138	0.189
	M9	2,1			0.003	0.241
	M19				−0.0030	0.222
	$\delta\phi/\delta x$		0.5020		0.3890	0.2915
	M9	2,2	0.5330		0.499	0.378
	M19		0.4896		0.4618	0.375

[a]Spanwise and chordwise grid points. [b]As reported in Ref. 21 using the method of Ref. 22. [c]As reported in Ref. 21 using the method of Ref. 13.

Table 3 AGARD arrow head wing (Fig. 3c) modes: $Z_1 = 1.0$, $Z_2 = X\text{-}C/2$, $AR = 4.0$

Mach No.	Methods (Matrix size or *Sp/Ch* Grid)[a]	*Qij*	$k=0$ *Re(Q)*	$k=0$ *Im(Q)*	$k=0.5$ *Re(Q)*	$k=0.5$ *Im(Q)*	$k=1.0$ *Re(Q)*	$k=1.0$ *Im(Q)*
	M9(34,15)[b]				0.059	0.6085	0.198	1.136
	M19(40,17)[c]	1,1			0.055	0.6122	0.186	1.144
	$\delta\phi/\delta x$(43)				0.046	0.6514	0.161	1.239
	M9(34,15)[b]		1.248		1.222	0.0766	1.164	0.190
	M19(40,17)[c]		1.255		1.228	0.0851	1.165	0.208
	$\delta\phi/\delta x$(43)	1,2	1.334		1.306	0.1318	1.254	0.292
2.0	M9(34,15)				0.031	0.226	0.105	0.406
	M19(40,17)	2,1			0.029	0.224	0.096	0.404
	$\delta\phi/\delta x$(43)				0.027	0.236	0.094	0.436
	M9(34,15)		0.471		0.457	0.0595	0.426	0.140
	M19(40,17)	2,2	0.467		0.452	0.0650	0.419	0.151
	$\delta\phi/\delta x$(43)		0.489		0.474	0.0858	0.448	0.188
	M9(34,35)				0.146	0.913		
	M19(26,26)	1,1			0.136	0.887		
	$\delta\phi/\delta x$(110)				0.146	1.104		
	M9(34,35)		2.002		1.911	0.138		
	M19(26,26)	1,2	1.936		1.852	0.147		
1.25	$\delta\phi/\delta x$(110)		2.182		2.316	0.156		
	M9(34,35)				0.075	0.330		
	M19(26,26)	2,1			0.072	0.329		
	$\delta\phi/\delta x$(110)				0.089	0.442		
	M9(34,35)		0.758		0.710	0.100		
	M19(26,26)		0.748		0.705	0.102		
	$\delta\phi/\delta x$(110)	2,2	0.858		0.949	0.101		

[a]Spanwise and chordwise grid points. [b]As reported in Ref. 21 using the method of Ref. 22. [c]As reported in Ref. 21 using the method of Ref. 13.

This implies that

$$K(X) = K(X_{TE})\, e^{i(k/\beta)(X - X_{TE})}$$

where $K(X_{TE})$ is the value of K at the trailing edge of the wing section being considered. If the wake is assumed to lie in the plane $Z=0$, its contribution to the normal modified velocity component can readily be deduced since

$$\frac{\delta K}{\delta X} = i\frac{k}{\beta} K(X_{TE})\, e^{i(k/\beta)(X - X_{TE})}$$

and $K(X_{TE})$ is the sum of the $\delta K/\delta X$ values for all the elements upstream.

Examples

To assess the solution accuracy and the versatility of the present potential gradient method, a limited number of calculations have been performed for three AGARD planforms (Fig. 3) and compared with the available results. The wing planforms were represented by trapezoidal finite elements. Generalized aerodynamic coefficients were calculated for heave and pitch modes for various reduced frequencies and Mach numbers. These results, in Tables 1, 2, and 3, are compared with Fenian's (M9, Ref. 22) and Stark's (M19, Ref. 13) as reported by Woodcock in Ref. 21. The number of elements (in chord/spanwise directions) used in each of the methods are shown within the parameters (see the tables). The generalized coefficients (Q_{ij}), from the present approach are seen to be in very good agreement with the referenced methods, in spite of the large differences in the matrix order.

Conclusions

The potential gradient approach results in, unlike the pressure potentials, simplified integral formulae. By expanding the kernel, the singular integrals have been evaluated in closed form without the need for principal or finite part integral techniques. Integrals vanish on the Mach cone and the need for determining the hyperbolic curves of intersection of the cone with the lifting surface is avoided. Furthermore, idealization of the lifting surface by trapezoidal finite elements with two sides parallel to the streamlines, requires line integrals to be performed along the other two sides only. Thus this approach is seen to be computationally very efficient.

Acknowledgment

This work is supported by NASA Contract No. NAS 1-13986 and R.W. Hess, NASA Langley Research Center, acted as the Technical Monitor.

References

[1] Jones, W. P., "Supersonic Theory for Oscillating Wings of Any Planform," A.R.CR&M 2655, June 1948.

[2] Giesing, J. P. Kalman, T. P., and Rodden, W. P., "Subsonic Unsteady Aerodynamics for General Configurations," USAF AFFDL-TR-71-5, Part I, Nov. 1971, AFFDL-TR-71-5, Part II, Air Force Flight Dynamics Lab., Wright-Patterson Air Force Base, Ohio, April 1972.

[3] Garrick, I. E. and Rubinow, S. I., "Theoretical Study of Air Forces on An Oscillating or Steady Thin Wing in a Supersonic Main Stream," NACA Rept. 827, 1947.

[4] Ashley, H., "Supersonic Airloads on Interfering Lifting Surfaces by Aerodynamic Influence Coefficient Theory," Rept. D2-22067, Nov. 1962, Boeing Aerospace Corp., Seattle, Wash.

[5] Watkins, C. E. and Berman, J. H., "On the Kernel Function of the Integral Equation Relating Lift and Downwash Distributions of Oscillating Wings in Supersonic Flow," NACA Rept. 1257, 1956.

[6] Harder, R. L. and Rodden, W. P., "Kernel Function for Non-Planar Oscillating Surfaces in Supersonic Flow," *Journal of Aircraft*, Vol. 8, Aug. 1971, pp. 667-679.

[7] Heaslet, M. A., Lomax, H., and Jones, A. L., "Volterra's Solution of the Wave Equation as Applied to Three-Dimensional Supersonic Airfoil Problems," NACA Rept. 889, 1947.

[8] Richardson, J. R., "A Method for Calculating the Lifting Forces on Wings (Unsteady Subsonic and Supersonic Lifting-Surface Theory)," Brit. A.R.C., R&M No. 3157, 1955.

[9] Cunningham, H. J., "Improved Numerical Procedure for Harmonically Deforming Lifting Surfaces from the Supersonic Kernel Function Method," *AIAA Journal*, Vol. 4, Nov. 1966, pp. 1961-1968.

[10] Cunningham, A. M., Jr., "A Kernel Function Method for Computing Steady and Oscillatory Supersonic Aerodynamics with Interference," AIAA Paper 73-670, Palm Springs, Calif., 1973.

[11] Ii, J. M., Boreland, C. J., and Hogley, J. R., "Prediction of Unsteady Aerodynamic Loadings of Non-Planar Wings and Wing-Tail Configurations in Supersonic Flow. Part I-Theoretical Development, Program Usage, and Application," USAF AFFDL-TR-71-108, Part I, Air Force Flight Dynamics Lab., Wright-Patterson Air Force Base, Ohio, March 1972.

[12] Kramer, G. D. and Kaylon, G. E., "Prediction of Unsteady Aerodynamic Loadings of Non-Planar Wings and Wing-Tail Configurations in Supersonic Flow. Part II," USAF AFFDL-TR-71-108, Part II, Air Force Flight Dynamics Lab., Wright-Patterson Air Force Base, Ohio, March 1972.

[13] Stark, V. J. E., "Calculation of Aerodynamic Forces on Two Oscillating Finite Wings at Low Supersonic Mach Numbers," SAAB Tech. Note TN 53, 1964.

[14] Appa, K., "Kinematically Consistent Unsteady Aerodynamic Coefficients in Supersonic Flow," *International Journal for Numerical Methods in Engineering*, Vol. 2, pp. 495-507, Oct. 1970; also National Aeronautical Laboratories NAL TN-9, India, March 1968.

[15] Appa, K. and Smith, G. C. C., "Further Developments in Consistent Unsteady Supersonic Aerodynamic Coefficients," *Journal of Aircraft*, Vol. 9, Feb. 1972.

[16] Appa, K. and Smith, G. C. C., "Development and Applications of Supersonic Unsteady Consistent Aerodynamics for Interfering Parallel Wings," NASA CR-2168, March 1973.

[17] Allen, D. J. and Sadler, D. S., "Oscillatory Aerodynamic Forces in Linearized Supersonic Flow for Arbitrary Frequencies, Planforms and Mach Numbers," Brit. A.R.C. R&M No. 3415, 1963.

[18] Woodcock, D. L. and York, E. J., "A Supersonic Box Collocation Method for the Calculation of Unsteady Airforces of Tandem Surfaces," *Proceedings of AGARD Symposium on Unsteady Aerodynamics for Aeroelastic Analyses of Interfering Surfaces*, AGARD-CP-80-71, 1971.

[19] Chen, L. T., Suciu, E. O., and Morino, L., "A Finite Element Method for Potential Aerodynamics Around Complex Configurations," AIAA Paper 74-107, Washington, D. C., 1974.

[20] Appa, K. and Smith, G. C. C., "Finite Element Approach to the Integrated Potential Formulation of General Unsteady Supersonic Aerodynamics," NASA-CR-112296, 1973.

[21] Woodcock, D. L. (ed.), "A Comparison of Methods Used in Lifting Surface Theory," Supplement to the Manual on Aeroelasticity, Pt. VI, NATO-AGARD Rept. No. 583, 1971.

[22] Fenain, M. and Guiraud-Vallee, D., "Numerical Calculations of Wings in Steady or Unsteady Supersonic Flow, Part 1: Steady Flow, Part 2: Unsteady Flow," Recherche Aperospatiale No. 115, 1966-67.

[23] Appa, K. and Jones, W. P., "Integrated Potential Formulation of Unsteady Supersonic Aerodynamics for Interacting Wings," presented at the AIAA 16th Structures, Structural Dynamics, and Materials (SDM) Conference, Denver, Colorado, May 27-29, 1975; to be published in the *Journal of Aircraft*.